Journal of the Neurological Sciences 368 (2016) 243–248

Contents lists available at ScienceDirect

Journal of the Neurological Sciences

journal homepage: www.elsevier.com/locate/jns

Loss of extra-striatal phosphodiesterase 10A expression in early premanifest Huntington's disease gene carriers

Heather Wilson [a], Flavia Niccolini [a], Salman Haider [b], Tiago Reis Marques [c], Gennaro Pagano [a], Christopher Coello [d], Sridhar Natesan [c], Shitij Kapur [c], Eugenii A. Rabiner [d,f], Roger N. Gunn [d,e], Sarah J. Tabrizi [b], Marios Politis [a,e,*]

[a] Neurodegeneration Imaging Group, Department of Basic and Clinical Neuroscience, Institute of Psychiatry, Psychology and Neuroscience, King's College London, London, UK
[b] Huntington's Disease Research Group, Department of Neurodegenerative Disease, Institute of Neurology, University College London, London, UK
[c] Department of Psychosis Studies, Institute of Psychiatry, Psychology and Neuroscience, King's College London, London, UK
[d] Imanova Ltd., Centre for Imaging Sciences, Hammersmith Hospital, London, UK
[e] Division of Brain Sciences, Department of Medicine, Imperial College London, London, UK
[f] Department of Neuroimaging, Institute of Psychiatry, Psychology and Neuroscience, King's College London, London, UK

ARTICLE INFO

Article history:
Received 8 March 2016
Received in revised form 5 July 2016
Accepted 12 July 2016
Available online 15 July 2016

Keywords:
Premanifest Huntington's disease
PDE10A
Insula
Occipital fusiform gyrus
PET
MRI

ABSTRACT

Huntington's disease (HD) is a monogenic neurodegenerative disorder with an underlying pathology involving the toxic effect of mutant huntingtin protein primarily in striatal and cortical neurons. Phosphodiesterase 10A (PDE10A) regulates intracellular signalling cascades, thus having a key role in promoting neuronal survival. Using positron emission tomography (PET) with [^{11}C]IMA107, we investigated the *in vivo* extra-striatal expression of PDE10A in 12 early premanifest HD gene carriers. Image processing and kinetic modelling was performed using MIAKAT™. Parametric images of [^{11}C]IMA107 non-displaceable binding potential (BP_{ND}) were generated from the dynamic [^{11}C]IMA107 scans using the simplified reference tissue model with the cerebellum as the reference tissue for nonspecific binding. We set a threshold criterion for meaningful quantification of [^{11}C]IMA107 BP_{ND} at 0.30 in healthy control data; regions meeting this criterion were designated as regions of interest (ROIs). MRI-based volumetric analysis showed no atrophy in ROIs. We found significant differences in mean ROIs [^{11}C]IMA107 BP_{ND} between HD gene carriers and healthy controls. HD gene carriers had significant loss of PDE10A within the insular cortex and occipital fusiform gyrus compared to healthy controls. Insula and occipital fusiform gyrus are important brain areas for the regulation of cognitive and limbic function that is impaired in HD. Our findings suggest that dysregulation of PDE10A-mediated intracellular signalling could be an early phenomenon in the course of HD with relevance also for extra-striatal brain areas.

1. Introduction

The intracellular enzyme phosphodiesterase 10A (PDE10A) is responsible for the hydrolysis of cyclic adenosine monophosphate (cAMP) and cyclic guanosine monophosphate (cGMP) and thus plays a role in regulating cyclic-nucleotide-mediated intracellular signalling cascades serving a number of gene transcription factors and neurotransmitter receptors [1]. PDE-10A has the potential to play a crucial role in mechanisms modulating motor, cognitive, and neuropsychiatric functions associated with Huntington's disease (HD). Recently, *in vivo* molecular imaging studies with PET have demonstrated 30–70% reduction of striatal PDE10A in HD gene carriers spanning from far onset premanifest [2] to near onset premanifest and early manifest [3] and advanced manifest [4] stages.

Although PDE10A is mainly expressed in striatal medium spiny neurons, previous work in wild-type and HD animal models have reported PDE10A protein expression in extra-striatal brain areas [5–7]. Evidence from human post-mortem data has shown that PDE10A immunoreactivity is detectable at low concentrations in extra-striatal regions including cortical neurons [7,8]. Furthermore, in experimental studies, PDE10A inhibition enhances cAMP response element-binding protein (CREB)-mediated signalling in cortical neurons of HD animal models indicating a direct effect of PDE10A on cortical neuronal survival [5,9]. Therefore, loss of extra-striatal PDE10A expression could be an important pathophysiological feature in the course of HD.

Abbreviations: BP_{ND}, Non-displaceable binding potential; cAMP, Cyclic adenosine monophosphate; CREB, CAMP-responsive element-binding protein; PDE10A, Phosphodiesterase 10 A; UHDRS, Unified Huntington's Disease Rating Scale.

* Corresponding author at: Neurodegeneration Imaging Group, Maurice Wohl Clinical Neuroscience Institute, 125 Coldharbour Lane, Camberwell, London SE5 9NU, UK.
E-mail address: marios.politis@kcl.ac.uk (M. Politis).

http://dx.doi.org/10.1016/j.jns.2016.07.033
0022-510X/

In this study, we assessed extra-striatal PDE10A expression in a group of normal controls using [^{11}C] IMA107 PET, aiming to identify brain areas where [^{11}C]IMA107 signal could be meaningfully quantified. Subsequently, we explored PDE10A expression, in those extra-striatal areas with measurable signal, in a group of early premanifest HD gene carriers. We hypothesised that extra-striatal areas that express quantifiable PDE10A levels *in vivo* could be altered early in HD.

2. Methods

2.1. Participants

Twelve early, far onset premanifest HD gene carriers were identified from the HD gene carrier registry database of National Hospital of Neurology and Neurosurgery, Queen Square, London. The time to symptom onset was estimated using a validated variant of the survival analysis formula, previously described [2]. All early premanifest HD gene carriers were clinically asymptomatic (Table 1). Twelve healthy individuals matched for age and gender served as the control group. Full inclusion and exclusion criteria previously reported [2]. Written informed consent was obtained from all study participants in accordance with the Declaration of Helsinki. The study was approved by the institutional review boards and the research ethics committee.

2.2. Clinical assessments

Motor function was assessed with the UHDRS TMS [10]. Functional capacity was assessed with clinician-based Total Functional Capacity scale (TFC), Independence Scale (IS), UHDRS functional assessment [10], and participant self-reported 36-Item Short Form Health Survey (SF-36) [11]. Neuropsychiatric symptoms were evaluated with the shortened form of the problem behaviour assessment (PBA) [12], the Beck Depression Inventory-II (BDI-II) [13], and the Hamilton Depression Rating Scale (HDRS) [14]. Cognitive assessments were carried out using the Cambridge Neuropsychological Test Automated Battery (CANTAB®). This incorporated assessments related to episodic memory (Paired Associate Learning), visual memory (Pattern Recognition Memory), attention (Reaction Time), executive function (One Touch Stockings of Cambridge), and language processing (Graded Naming Test).

2.3. Scanning procedures

PET and MR imaging was performed at Imanova Ltd., London, UK. Details of PET and MRI scanners have been described previously [2]. In brief, following an intravenous bolus mean dose of ±258 MBq [^{11}C]IMA107, PET scans were obtained on a Biograph Hi-Rez 6 PET-CT scanner (Siemens) by acquiring dynamic emission data continuously for 90 min. All participants were scanned after withholding consumption of caffeinate beverages for 12 h [15]. MRI scans included T1-weighted magnetization prepared rapid acquisition with gradient echo sequence (MPRAGE), for co-registration with PET images, acquired with a 32-channel head coil on a Siemens Magnetom Verio 3-T MRI scanner. All sequences used a 1 mm^3 voxel size, anteroposterior phase encoding direction, and a symmetric echo.

Table 1
Clinical characteristics of early premanifest HD gene carriers and healthy controls.

	Healthy controls	Premanifest HD gene carriers
No	12	12
Sex	9 M/3F	7 M/5F
Age (years ± SD)	39.8 (±1.9)	41.2 (±7.5)
CAG repeats (±SD) [range]	–	41.8 (±1.3) [40–44]
Disease Burden Score[1] (±SD) [range]	–	254.4 (±46.8) [153–323]
90% probability to onset[2] (years ± SD) [range]	–	25.0 (±6.9) [17–43]
UHDRS TMS[3] (±SD)	0 (±0)	0 (±0)
UHDRS DCL[4] (±SD)	–	0 (±0)

[1] Disease burden score: age X (CAG length–35·5).
[2] 90% probability to onset = predicted years to Huntington's disease symptoms onset (90% probability) calculated on the basis of variant of the survival analysis formula described by [2].
[3] Unified Huntington Disease Rating Scale Total Motor Score (UHDRS TMS).
[4] Unified Huntington Disease Rating Scale Diagnostic Confidence Level (UHDRS DCL).

2.4. Imaging data analysis

Image processing and kinetic modelling was carried out using the Molecular Imaging and Kinetic Analysis Toolbox software package (MIAKAT™: www.miakat.org; [16], which also uses software from SPM12 (Wellcome Trust Centre for Neuroimaging) and FSL (FMRIB, University of Oxford) and is implemented in MATLAB® (The Mathworks, Natick, MA, USA). The MIAKAT processing pipeline was followed, ensuring all quality control steps were completed to generate both parametric images and regional estimates of [^{11}C]IMA107 BP_{ND}.

Appropriate brain extraction fractional intensity threshold was selected and applied to the individual isotopic MRI, using the FSL Brain Extraction Tool [17]. The T1-weighted MR image was segmented into white matter, grey matter, and cerebrospinal fluid. Normalisation of the T1 MR image into stereotaxic space enabled non-linear registration between template brain MRI [Montreal Neurological Institute (MNI)-152 template], stereotaxic neuroanatomical CIC atlas version 1.2 [18], and the individual subject. All images were checked following spatial normalization to ensure registration accuracy. Individual PET frames were corrected for head motion using frame-by-frame rigid registration using a frame with high signal-to-noise ratio as reference. PET images were anatomically co-registered and to the corresponding MPRAGE MRI and subsequently spatially normalised into the T1-weighted MNI space.

Parametric images of [^{11}C]IMA107 non-displaceable binding potential (BP_{ND}) were generated from the dynamic [^{11}C]IMA107 scans using a basis function implementation of the simplified reference tissue model (SRTM) [19], with the cerebellum as the reference tissue. Previous PET studies have shown lower PDE10A uptake in the cerebellum [20] and a blocking study with selective PDE10A inhibitors has shown no changes in cerebellar [^{11}C]IMA107 binding (Imanova internal data), confirming the suitability of the cerebellum as a reference region for the determination of the regional estimation of BP_{ND}.

2.5. Region of interest analysis

The anatomical CIC atlas version 1.2 [18] was used to define ROIs. This atlas consists of a total of 119 regions; cortical regions are modified from the Harvard–Oxford atlas, subcortical regions defined on the non-linear ICM152 template following MAN I guidelines and the thalamus replaced by thalamic connectivity atlas obtained from FMRIB, Oxford University [18,20]. Regional time-activity data for ROIs was derived from dynamic PET data and regional BP_{ND} estimates obtained using the SRTM model with the cerebellum as the reference region. To ensure sufficient PDE10A expression, a threshold of healthy control mean regional [^{11}C]IMA107 $BP_{ND} > 0.30$ was applied. Regions with average healthy control [^{11}C]IMA107 $BP_{ND} \leq 0.30$ were excluded from statistical analysis.

2.6. MRI volumetric analysis

Since PDE10A is an intracellular enzyme, neuronal loss may affect its expression. We investigated volumetric changes in extra-striatal regions in our cohort of premanifest HD gene carriers compared to healthy controls. Volumetric ROIs were bilaterally defined on each subjects volumetric T1-weighted MRI using the CIC v1.2 atlas. Volumes were extracted and corrected for total intracranial volume using validated methods [22].

2.7. Statistical analysis

Statistical analysis and graphical representations of data were performed with SPSS (SPSS version 21.0, Chicago, Illinois, USA) and GraphPad Prism (version 6.0 c). For all variables, homogeneity and Gaussianity were tested with Bartlett and Kolmogorov–Smirnov tests. We investigated for possible outliers using the ROUT test in GraphPad Prism, with maximum desired false discovery rate (FDR) set to 1% [23]. Any outliers were removed prior to further statistical analysis. Multivariate analysis of variance (MANOVA) was used to assess the overall effects of extra-striatal regional [^{111}C]IMA107 BP_{ND} between groups of premanifest HD gene carriers and healthy controls, reporting Pillai's Trace *P* value. Independent parametric (*t*-test) and non-parametric (Mann–Whitney *U*) tests, followed by Bonferroni's correction for multiple comparisons were used to assess effects of extra-striatal ROI [^{11}C]IMA107 BP_{ND} between the two groups. We interrogated correlations between PET and clinical data and between extra-striatal and striatal [^{11}C]IMA107 BP_{ND}, using Spearman's r_s and applied the Benjamini–Hochberg correction to reduce the false discovery rate [24]. The false discovery rate cut-off was set at 0.05. For all comparisons, the level α was set at $P < 0.05$; all data presented as mean ± SD.

3. Results

3.1. Clinical measures

No significant differences were found between early premanifest HD gene carriers and healthy controls in motor and functional ($P > 0.10$), neuropsychiatric ($P > 0.10$) and cognitive ($P > 0.10$) assessments (previously reported (2)).

3.2. MRI volumetric analysis

Grey and white matter volumetric brain changes have been reported as one of the earliest changes in HD [25] with volumetric changes occurring in cortical regions [26,27]. Therefore, it was important to identify if the cohort of premanifest HD gene carriers had significant volumetric changes, which could be a potential confounding factor when measuring intracellular PDE10A expression. MRI volumetric analysis confirmed there was no significant volume change in any extra-striatal regions between the groups of early premanifest HD gene carriers and healthy controls ($P > 0.10$) (Supplementary Table S1).

3.3. Extra-striatal PDE10A expression

Extra-striatal brain regions meeting the threshold criteria in healthy controls, [^{11}C]IMA107 $BP_{ND} > 0.30$, included insular cortex, occipital fusiform gyrus, occipital pole, and posterior cingulate gyrus (Table 2, Fig. 1a).

We found significant differences in mean extra-striatal [^{11}C]IMA107 BP_{ND} between the early premanifest HD gene carriers and healthy controls groups ($P = 0.013$). Early premanifest HD gene carriers had significantly decreased mean [^{11}C]IMA107 BP_{ND} in the insular cortex ($P = 0.029$; −25.1%) (Fig. 1b, Fig. 2) and in the occipital fusiform gyrus ($P = 0.003$; −41.9%) (Fig. 1c) compared to the healthy controls.

[^{11}C]IMA107 BP_{ND} value for one healthy control subject in the occipital fusiform gyrus was identified as outliers and removed. Two early premanifest HD gene carriers displayed negative [^{11}C]IMA107 BP_{ND} values in the insular cortex, these values were removed from the HD gene carrier group in the insula only. Removal of these values did not affect the significance level.

We investigated possible association between PDE10A expression and clinical measures; however, no significant correlation between [^{11}C]IMA107 BP_{ND} and clinical data were identified in any regions.

To confirm the [^{11}C]IMA107 signal detected in the insula and occipital fusiform gyrus specifically measured PDE10A enzyme, and not just background noise, we looked for correlations with [^{11}C]IMA107 signal in striatal regions where PDE10A is known to be highly expressed [2]. We found significant positive correlations between loss of [^{11}C]IMA107 BP_{ND} in the insula with loss of [^{11}C]IMA107 BP_{ND} in the striatum ($r_s = 0.733$; $P < 0.001$), caudate ($r_s = 0.711$; $P < 0.001$), globus pallidus ($r_s = 0.573$; $P = 0.006$), and putamen ($r_s = 0.726$; $P < 0.001$) (Fig. 3A); signal loss in the occipital fusiform gyrus also significantly correlated with signal loss in the striatum ($r_s = 0.575$; $P = 0.010$), caudate ($r_s = 0.534$; $P = 0.015$), globus pallidus ($r_s = 0.428$; $P = 0.042$), and putamen ($r_s = 0.608$; $P = 0.010$) (Fig. 3B).

4. Discussion

Using non-invasive imaging, we demonstrated significant loss of extra-striatal PDE10A expression, specifically 25% loss in the insular cortex and 42% loss in the occipital fusiform gyrus, in early premanifest HD gene carriers who were several years before their predicted symptomatic onset. We did not detect significant volume change in our HD gene carriers, indicating that [^{11}C]IMA107 BP_{ND} loss reported here is not due to regional atrophy. Previous work has shown the importance of PDE10A in the pathophysiology of HD, in particular the loss of striatal PDE10A in premanifest and manifest stages of HD [2–4]. The current study demonstrates altered PDE10A expression beyond the basal ganglia, early in the course of the disease, and supports PDE10A as potentially one of the earliest pathophysiological features of HD.

The insula and occipital fusiform gyrus are key regions associated with the development of cognitive and limbic functions [27–30]. Imaging studies have previously demonstrated changes in the insula, occipital, and fusiform cortex in premanifest and symptomatic HD. PET studies have reported increased microglial activation [31,32] and loss of D_2/D_3 dopamine receptor availability [33] in the insular cortex of premanifest and manifest HD gene carriers. PET with [^{18}F]flurodeoxyglucose showed loss of metabolic activity in the insula while the occipital cortex showed increased metabolic activity in early premanifest HD gene carriers [34]. fMRI studies report reduced neural activity in the insula of early premanifest HD [35] and reduced neuronal activity within the fusiform cortex [28] and occipital cortex [36] in early manifest HD. Results from the present study suggest dysregulation of PDE10A also occurs in the insula and occipital fusiform gyrus; however, the relationship between these pathophysiological events is currently unknown.

PDE10A has a key role in regulating intracellular signalling and given the functional significance of the insula and occipital fusiform gyrus, loss of PDE10A expression reported here could be an early phenomenon underlying subsequent development of cognitive and behavioural symptoms in the course of HD. In our study, we did not find associations between loss of PDE10A expression in the insula or occipital fusiform gyrus and cognitive and behavioural performance as measured by specialised tools. However, our sample size was relatively small and premanifest HD gene carriers at a far onset stage with intact brain functions. Our design is limited due to the cross-sectional nature; however, it could be possible that future prospective studies may show that loss of

Table 2
[^{11}C]IMA107 BP_{ND} in anatomically defined regions comparing healthy controls and early premanifest HD gene carriers.

Extra-striatal regions of interest	Healthy controls	Premanifest HD gene carrier	*P* value*	% change in pHD
Insular cortex	0.34 (±0.1)	0.26 (±0.1)	**0.029**	−25.1
Occipital Fusiform gyrus	0.37 (±0.1)	0.21 (±0.1)	**0.003**	−41.9
Occipital Pole	0.35 (±0.1)	0.34 (±0.1)	>0.10	−2.7
Posterior Cingulate gyrus	0.38 (±0.2)	0.32 (±0.1)	>0.10	−17.6

Selected regions with control [^{11}C]IMA107 $BP_{ND} > 0.30$.
Negative percentage change indicates lower PDE10A expression in premanifest HD gene carriers compared to controls.
In the table bold font highlights significant P values ($P < 0.05$).
* *P* values are Bonferroni corrected.

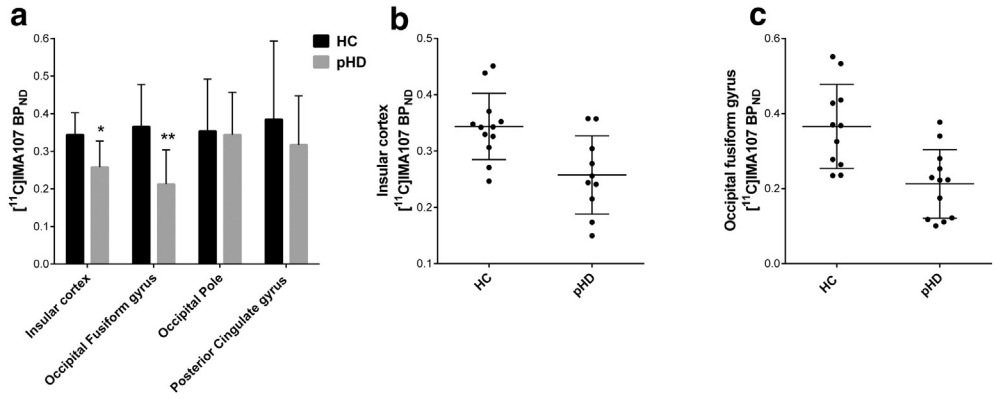

Fig. 1. Loss of PDE10A expression in the insular cortex and occipital fusiform gyrus in early premanifest HD gene carriers. (*a*) Column bar graph showing mean [^{11}C]IMA107 BP_{ND} extra-striatal regions with control $BP_{ND} > 0.30$ for healthy controls (HC) and premanifest HD gene carriers (pHD). Bonferroni corrected $^{*}P < 0.05$, $^{**}P < 0.01$. Scatterplots showing distribution of individual BP_{ND} values in the insular cortex (*b*) and the occipital fusiform gyrus (*c*). Error bars represent mean ± standard deviation (SD).

PDE10A expression in the insula and occipital fusiform gyrus are associated with the risk of developing cognitive and behavioural issues in manifest HD. Furthermore, in HD, the affected extra-striatal regions could play a role in visuomotor [37], visuospatial [38], and oculomotor [39,40], as well as facial expression deficits [41,42]. In the present study, we did not examine visual function or face recognition. Therefore, further studies with specific clinical measures assessing such deficits may highlight clinical associations.

To support the reliability of our data, we demonstrated that loss of [^{11}C]IMA107 signal in the insula and occipital fusiform gyrus correlated with loss of [^{11}C]IMA107 signal in striatal regions; striatal loss of PDE10A signal has been previously reported [2]. Further work is needed to fully validate the use of the cerebellum as a reference region for quantification of low [^{11}C]IMA107 signal detected in extra-striatal regions and estimate the level of specific compared to nonspecific binding. Moreover, alternative higher affinity ligands such as [^{11}C]IMA106 [20] may facilitate the imaging extra-striatal regions, further confirming the reliability of extra-striatal BP_{ND} values presented here.

A recent 1 year follow-up study demonstrated a mean annual loss of PDE10A of 16.6% in the caudate, 6.9% in the putamen, and 5.8% in the globus pallidus [43]. Furthermore, two genetic studies have identified PDE10A mutations as a cause of hyperkinetic movement disorders [44,45] confirming the role of PDE10A in regulating striato-cortical activity and supporting an important role of PDE10A in the pathophysiology of HD. Findings that PDE10A changes can be detected outside the striatum, even at early premanifest stages, further increase the value of PDE01A as a biomarker to track disease progression in HD.

In conclusion, we provide *in vivo* evidence for the loss of PDE10A expression in insula and occipital fusiform gyrus a number of years before symptomatic onset in premanifest HD gene carriers. Further studies are needed to explore the relevance of extra-striatal PDE10A loss in the development of cognitive and behavioural symptoms. This study supports the increasing evidence for the role of PDEs in neurodegenerative disorders and the use of [^{11}C]IMA107 PET as a robust imaging tool to study PDE10A *in vivo* in the human brain and disease.

Supplementary data to this article can be found online at http://dx.doi.org/10.1016/j.jns.2016.07.033.

Conflict of interest

On behalf of all authors, the corresponding author states that there is no conflict of interest.

Funding

This research was financially supported by the National Institute for Health Research (NIHR) Mental Health Biomedical Research Centre at South London and Maudsley NHS Foundation Trust and King's College London, and the NIHR Biomedical Research Centre at Imperial College London. The views expressed are those of the authors and not necessarily those of the NHS, the NIHR, or the Department of Health. Marios Politis research is supported by Parkinson's UK, Edmond J. Safra Foundation, Michael J Fox Foundation (MJFF), and NIHR BRC.

Acknowledgments

We thank all participants and their families, the PET technicians and radiochemists, the MRI radiographers, and the clinical research nurses at Imanova Ltd. for their cooperation and support to this study. We also thank Nicola Robertson and Clare Loane for assisting with the

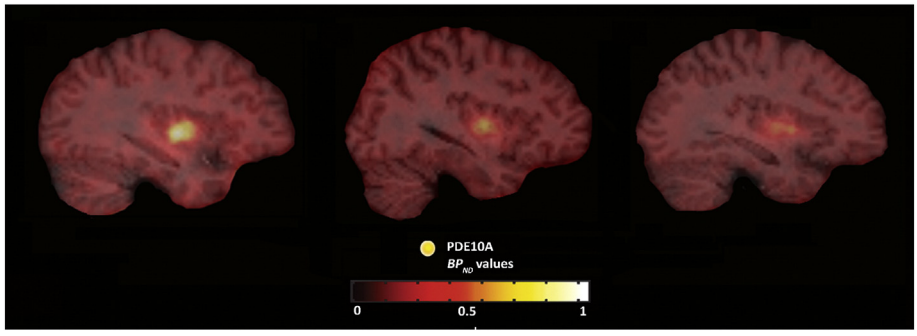

Fig. 2. Significant loss of PDE10A within the insular cortex in premanifest HD gene carriers compared to healthy controls. Sagittal summed [^{11}C]IMA107 PET images co-registered and fused with 3-T MRI images for the insula of a 40-year-old female showing normal insula [^{11}C]IMA107 binding ($BP_{ND} = 0.451$) (left); a 43-year-old male premanifest HD gene carrier (CAGr: 43; DBS: 322.5; 17 years from predicted onset) showing moderate decreased insula [^{11}C]IMA107 binding ($BP_{ND} = 0.215$) (middle); a 44-year-old male premanifest HD gene carrier (CAGr: 41; DBS: 236.5; 27 years from predicted onset) showing severe decreased insula [^{11}C]IMA107 binding ($BP_{ND} = 0.173$) (right). Colour bar reflects range of [^{11}C]IMA107 BP_{ND} intensity.

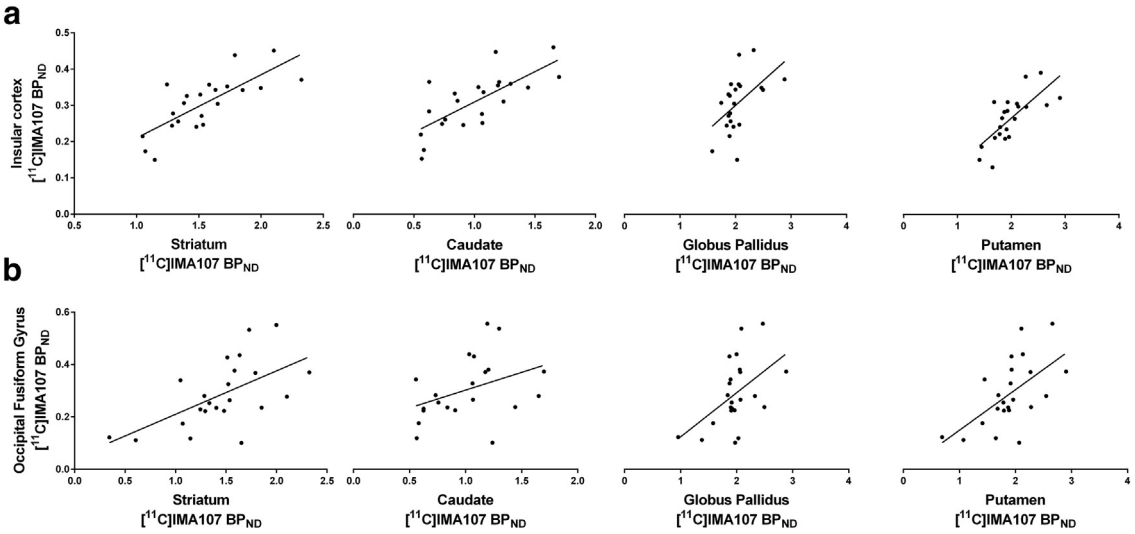

Fig. 3. Correlation between [^{11}C]IMA107 BP_{ND} in anatomically defined extra-striatal and striatal regions of interest. Loss [^{11}C]IMA107 BP_{ND} in (*A*) the insular cortex correlated with loss of [^{11}C]IMA107 BP_{ND} in the striatum ($r_s = 0.733$; $P < 0.001$), caudate ($r_s = 0.711$; $P < 0.001$), globus pallidus ($r_s = 0.573$; $P = 0.006$), and putamen ($r_s = 0.726$; $P < 0.001$); (*B*) the occipital fusiform gyrus correlated with loss of [^{11}C]IMA107 BP_{ND} in the striatum ($r_s = 0.575$; $P = 0.010$), caudate ($r_s = 0.534$; $P = 0.015$), globus pallidus ($r_s = 0.428$; $P = 0.042$), and putamen ($r_s = 0.608$; $P = 0.010$).

recruitment of Huntington's disease gene carriers and for demonstrating CANTAB®, respectively.

References

[1] A. Nishi, M. Kuroiwa, D.B. Miller, J.P. O'Callaghan, H.S. Bateup, T. Shuto, et al., Distinct roles of PDE4 and PDE10A in the regulation of cAMP/PKA signaling in the striatum, J. Neurosci. 28 (42) (2008) 10460–10471.

[2] F. Niccolini, S. Haider, T. Reis Marques, N. Muhlert, A.C. Tziortzi, G.E. Searle, et al., Altered PDE10A expression detectable early before symptomatic onset in Huntington's disease, Brain 138 (2015) 3016–3029.

[3] D.S. Russell, O. Barret, D.L. Jennings, J.H. Friedman, G.D. Tamagnan, D. Thomae, et al., The phosphodiesterase 10 positron emission tomography tracer, F-18 MNI-659, as a novel biomarker for early Huntington disease, JAMA Neurol. 71 (12) (2014) 1520–1528.

[4] R. Ahmad, S. Bourgeois, A. Postnov, M.E. Schmidt, G. Bormans, K. Van Laere, et al., PET imaging shows loss of striatal PDE10A in patients with Huntington disease, Neurology 82 (3) (2014) 279–281.

[5] A. Giralt, A. Saavedra, O. Carreton, H. Arumi, S. Tyebji, J. Alberch, et al., PDE10 inhibition increases GluA1 and CREB phosphorylation and improves spatial and recognition memories in a Huntington's disease mouse model, Hippocampus 23 (8) (2013) 684–695.

[6] A. Saavedra, A. Giralt, H. Arumi, J. Alberch, E. Perez-Navarro, Regulation of hippocampal cGMP levels as a candidate to treat cognitive deficits in Huntington's disease, Plos One 8 (9) (2013).

[7] T.F. Seeger, B. Bartlett, T.M. Coskran, J.S. Culp, L.C. James, D.L. Krull, et al., Immunohistochemical localization of PDE10A in the rat brain, Brain Res. 985 (2) (2003) 113–126.

[8] T.M. Coskran, D. Morton, F.S. Menniti, W.O. Adamowicz, R.J. Kleiman, A.M. Ryan, et al., Immunohistochemical localization of phosphodiesterase 10A in multiple mammalian species, J. Histochem. Cytochem. 54 (11) (2006) 1205–1213.

[9] C. Giampa, D. Laurenti, S. Anzilotti, G. Bernardi, F.S. Menniti, F.R. Fusco, Inhibition of the striatal specific phosphodiesterase PDE10A ameliorates striatal and cortical pathology in R6/2 mouse model of Huntington's disease, Plos One 5 (10) (2010).

[10] The Huntington Study Group, The Unified Huntington's Disease Rating Scale: reliability and consistency, Mov. Disord. 11 (2) (1996) 136–142.

[11] C.A. McHorney, J.E. Ware, A.E. Raczek, The MOS 36-item short-form health survey (SF-36) 0.2. Psychometric and clinical-tests of validity in measuring physical and mental-health constructs, Med. Care 31 (3) (1993) 247–263.

[12] D. Craufurd, J.C. Thompson, J.S. Snowden, Behavioral changes in Huntington disease, Neuropsychiatry Neuropsychol. Behav. Neurol. 14 (4) (2001) 219–226.

[13] A. Beck, G. Steer, Brown, Beck Depression Inventory-II (BDI-II): manual for Beck Depression Inventory-II, Pearson, 1993.

[14] M. Hamilton, A rating scale for depression, J. Neurol. Neurosurg. Psychiatry 23 (1) (1960) 56–62.

[15] B.B. Fredholm, K. Battig, J. Holmen, A. Nehlig, E.E. Zvartau, Actions of caffeine in the brain with special reference to factors that contribute to its widespread use, Pharmacol. Rev. 51 (1) (1999) 83–133.

[16] G. Searle, C. Coello, R. Gunn, Realising the binding potential directly and indirectly, J. Cereb. Blood Flow Metab. (2015) (BrainPET supplement 64 Brain 0791:19–20).

[17] S.M. Smith, Fast robust automated brain extraction, Hum. Brain Mapp. 17 (3) (2002) 143–155.

[18] A.C. Tziortzi, G.E. Searle, S. Tzimopoulou, C. Salinas, J.D. Beaver, M. Jenkinson, et al., Imaging dopamine receptors in humans with C-11-(+)-PHNO: dissection of D3 signal and anatomy, NeuroImage 54 (1) (2011) 264–277.

[19] R.N. Gunn, A.A. Lammertsma, S.P. Hume, V.J. Cunningham, Parametric imaging of ligand-receptor binding in PET using a simplified reference region model, NeuroImage 6 (4) (1997) 279–287.

[20] C. Plisson, D. Weinzimmer, S. Jakobsen, S. Natesan, C. Salinas, S.-F. Lin, et al., Phosphodiesterase 10A PET radioligand development program: from pig to human, J. Nucl. Med. 55 (4) (2014) 595–601.

[21] H. Johansen-Berg, T.E. Behrens, E. Sillery, O. Ciccarelli, A.J. Thompson, S.M. Smith, et al., Functional-anatomical validation and individual variation of diffusion tractography-based segmentation of the human thalamus, Cereb. Cortex 15 (1) (2005) 31–39.

[22] R.L. Buckner, D. Head, J. Parker, A.F. Fotenos, D. Marcus, J.C. Morris, et al., A unified approach for morphometric and functional data analysis in young, old, and demented adults using automated atlas-based head size normalization: reliability and validation against manual measurement of total intracranial volume, NeuroImage 23 (2) (2004) 724–738.

[23] H.J. Motulsky, R.E. Brown, Detecting outliers when fitting data with nonlinear regression—a new method based on robust nonlinear regression and the false discovery rate, BMC Bioinforma. 7 (2006).

[24] Y. Benjamini, Y. Hochberg, Controlling the false discovery rate: a practical and powerful approach to multiple testing, J. R. Stat. Soc. 57 (1) (1995) 289–300.

[25] S.J. Tabrizi, D.R. Langbehn, B.R. Leavitt, R.A.C. Roos, A. Durr, D. Craufurd, et al., Biological and clinical manifestations of Huntington's disease in the longitudinal TRACK-HD study: cross-sectional analysis of baseline data, Lancet Neurol. 8 (9) (2009) 791–801.

[26] G. Douaud, V. Gaura, M.J. Ribeiro, F. Lethimonnier, R. Maroy, C. Verny, et al., Distribution of grey matter atrophy in Huntington's disease patients: a combined ROI-based and voxel-based morphometric study, NeuroImage 32 (4) (2006) 1562–1575.

[27] H.D. Rosas, D.H. Salat, S.Y. Lee, A.K. Zaleta, V. Pappu, B. Fischl, et al., Cerebral cortex and the clinical expression of Huntington's disease: complexity and heterogeneity, Brain 131 (2008) 1057–1068.

[28] R.C. Wolf, F. Sambataro, N. Vasic, M.S. Depping, P.A. Thomann, G.B. Landwehrmeyer, et al., Abnormal resting-state connectivity of motor and cognitive networks in early manifest Huntington's disease, Psychol. Med. 44 (15) (2014) 3341–3356.

[29] D.L. Harrington, M. Rubinov, S. Durgerian, L. Mourany, C. Reece, K. Koenig, et al., Network topology and functional connectivity disturbances precede the onset of Huntington's disease, Brain 138 (Pt 8) (2015) 2332–2346.

[30] A. Peinemann, S. Schuller, C. Pohl, T. Jahn, A. Weindl, J. Kassubek, Executive dysfunction in early stages of Huntington's disease is associated with striatal and insular atrophy: a neuropsychological and voxel-based morphometric study, J. Neurol. Sci. 239 (1) (2005) 11–19.

[31] Y.F. Tai, N. Pavese, A. Gerhard, S.J. Tabrizi, R.A. Barker, D.J. Brooks, et al., Microglial activation in presymptomatic Huntington's disease gene carriers, Brain 130 (2007) 1759–1766.

[32] M. Politis, N. Pavese, Y.F. Tai, L. Kiferle, S.L. Mason, D.J. Brooks, et al., Microglial activation in regions related to cognitive function predicts disease onset in Huntington's disease: a multimodal imaging study, Hum. Brain Mapp. 32 (2) (2011) 258–270.

[33] N. Pavese, M. Politis, Y.F. Tai, R.A. Barker, S.J. Tabrizi, S.L. Mason, et al., Cortical dopamine dysfunction in symptomatic and premanifest Huntington's disease gene carriers, Neurobiol. Dis. 37 (2) (2010) 356–361.

[34] A. Feigin, K.L. Leenders, J.R. Moeller, J. Missimer, G. Kuenig, P. Spetsieris, et al., Metabolic network abnormalities in early Huntington's disease: an F-18 FDG PET study, J. Nucl. Med. 42 (11) (2001) 1591–1595.

[35] J.L. Zimbelman, J.S. Paulsen, A. Mikos, N.C. Reynolds, R.G. Hoffmann, S.M. Rao, fMRI detection of early neural dysfunction in preclinical Huntington's disease, J. Int. Neuropsychol. Soc. 13 (5) (2007) 758–769.
[36] V.P. Clark, S. Lai, A.W. Deckel, Altered functional MRI responses in Huntington's disease, Neuroreport 13 (5) (2002) 703–706.
[37] B.F. O'Donnell, T.M. Blekher, M. Weaver, K.M. White, J. Marshall, X. Beristain, et al., Visual perception in prediagnostic and early stage Huntington's disease, J. Int. Neuropsychol. Soc. 14 (3) (2008) 446–453.
[38] A.D. Lawrence, L.H.A. Watkins, B.J. Sahakian, J.R. Hodges, T.W. Robbins, Visual object and visuospatial cognition in Huntington's disease: implications for information processing in corticostriatal circuits, Brain 123 (2000) 1349–1364.
[39] J.P. Morris, G. McCarthy, Guided saccades modulate object and face-specific activity in the fusiform gyrus, Hum. Brain Mapp. 28 (8) (2007) 691–702.
[40] T. Blekher, S.A. Johnson, J. Marshall, K. White, S. Hui, M. Weaver, et al., Saccades in presymptomatic and early stages of Huntington disease, Neurology 67 (3) (2006) 394–399.
[41] A. Hennenlotter, U. Schroeder, P. Erhard, B. Haslinger, R. Stahl, A. Weindl, et al., Neural correlates associated with impaired disgust processing in pre-symptomatic Huntington's disease, Brain 127 (Pt 6) (2004) 1446–1453.
[42] S.M. Henley, E.J. Wild, N.Z. Hobbs, J.D. Warren, C. Frost, R.I. Scahill, et al., Defective emotion recognition in early HD is neuropsychologically and anatomically generic, Neuropsychologia 46 (8) (2008) 2152–2160.
[43] D.S. Russell, D.L. Jennings, O. Barret, G.D. Tamagnan, V.M. Carroll, F. Caille, et al., Change in PDE10 across early Huntington disease assessed by [18F]MNI-659 and PET imaging, Neurology 86 (8) (2016) 748–754.
[44] N.E. Mencacci, E.J. Kamsteeg, K. Nakashima, L. R'Bibo, D.S. Lynch, B. Balint, et al., De novo mutations in PDE10A cause childhood-onset chorea with bilateral striatal lesions, Am. J. Hum. Genet. 98 (4) (2016) 763–771.
[45] C.P. Diggle, S.J. Sukoff Rizzo, M. Popiolek, R. Hinttala, J.P. Schulke, M.A. Kurian, et al., Biallelic mutations in PDE10A lead to loss of striatal PDE10A and a hyperkinetic movement disorder with onset in infancy, Am. J. Hum. Genet. 98 (4) (2016) 735–743.